Direct Observation and Structural Characterization of the Encounter Complex in Bimolecular Electron Transfers with Photoactivated Acceptors

R. Rathore, S. M. Hubig, and J. K. Kochi*

Contribution from the Department of Chemistry, University of Houston, Houston, Texas 77204-5641

Received April 14, 1997[⊗]

Abstract: The encounter complex between photoexcited quinones Q* and various aromatic donors (ArH) is observed directly by time-resolved ps spectroscopy immediately before it undergoes electron transfer to the ion-radical pair [$Q^{\bullet-}$, $ArH^{\bullet+}$]. The encounter complex (EC) is spectrally characterized by distinctive (near IR) absorption bands, and its temporal evolution is established by quantitative kinetics analysis. The structural characterization of the 1:1 encounter complex [Q*, ArH] identifies the cofacial juxtaposition of the donor and acceptor moieties for optimal overlap of their π-orbitals. Further comparisons of the (excited-state) encounter complex with the corresponding (ground-state) EDA complex of aromatic donors and quinones establish its charge-transfer character, which directly relates to electron transfer within the encounter complex. The mechanistic significance of the encounter complex to bimolecular electron transfer is discussed (Scheme 1).

Introduction

Bimolecular electron transfer between a freely diffusing electron donor (D) and an acceptor (A) requires the intervention of a precursor or encounter complex immediately prior to electron exchange,[1] and theoretical analyses uniformly incorporate such an intermolecular complex [D,A] to accommodate the Franck−Condon requirement for ultrafast electron jump.[2,3] However, experimental confirmation has lagged the theoretical constructs and little is definitively known about the postulated encounter complexes[4]—in particular, how their formation, lifetime, structure, and electronic configuration affect the overall electron-transfer rates.

Time-resolved picosecond spectroscopy now provides the means to detect even short-lived (transient) species and to follow their temporal evolution in real time.[5] Indeed, we believe the exploitation of laser-flash techniques will allow the collisional course of a photoactived electron acceptor A* to be monitored directly as it evolves with an electron donor (D) to the transient complex prior to electron transfer, *i.e.*

$$A^* + D \rightleftharpoons [\text{complex}] \rightarrow A^{\bullet-} + D^{\bullet+} \qquad (1)$$

Various experimental approaches to elucidate photoinduced electron transfer have led to the discovery of a variety of short-lived intermediates such as excited charge-transfer complexes,[6] exciplexes,[7] contact ion-radical pairs,[8] solvent-separated ion-radical pairs,[9] free ion radicals, etc., which have been detected by time-resolved absorption and emission measurements. However, the relationships among the various intermediates and their temporal sequence in the electron-transfer mechanism are not clear. For example, Gould, Farid, and co-workers[10] showed convincingly by quantitative fluorescence measurements that exciplexes or excited charge-transfer complexes are common intermediates in a series of bimolecular electron-transfer reactions in different solvents. However, the emission data did not allow the authors to establish the temporal sequence in the formation of exciplexes and solvent-separated ion pairs in polar solvents.

The discussion of whether exciplexes or excited charge-transfer complexes are involved in electron-transfer quenching reactions reached its first critical stage about three decades ago, when the Rehm−Weller relationship between the fluorescence quenching rate constants and the electron-transfer driving force in polar solvents was introduced.[11] This free-energy correlation was based on a purely "outer-sphere" electron-transfer model that explicitly excluded the consideration of an excited charge-transfer complex as an intermediate, as postulated earlier by Mataga *et al.*[12] The role of exciplexes or excited charge-transfer complexes as intermediates in electron transfer processes has been actively discussed since then,[10,13,14] and the question of

[⊗] Abstract published in *Advance ACS Abstracts,* November 1, 1997.

(1) (a) Libby, W. F. *J. Phys. Chem.* **1952**, *56*, 863. (b) Laidler, K. J. *Can. J. Chem.* **1959**, *37*, 138. (c) Rabinovich, E. *Trans. Faraday Soc.* **1937**, *33*, 1225. (d) For the concept of encounter-complex formation in bimolecular reactions, see: Eigen, M. *Angew. Chem., Int. Ed. Engl.* **1964**, *3*, 1.

(2) (a) Marcus, R. A. *J. Chem. Phys.* **1956**, *24*, 966. (b) Hush, N. S. *Trans. Faraday Soc.* **1961**, *57*, 557.

(3) For reviews, see: (a) Cannon, R. D. *Electron Transfer Reactions;* Butterworths: London, 1980. (b) Bolton, J. R.; Mataga, N.; McLendon, G. *Electron Transfer in Inorganic, Organic and Biological Systems*; American Chemical Society: Washington, DC, 1991.

(4) Sutin, N. *Acc. Chem. Res.* **1968**, *1*, 225.

(5) For example see: (a) West, M. A. In *Creation and Detection of the Excited State*; Ware, W. R., Ed.; Marcel Dekker: New York, 1976; p 218. (b) Simon, J. D. *Rev. Sci. Instrum.* **1989**, *60*, 3597.

(6) Ottolenghi, M. *Acc. Chem. Res.* **1973**, *6*, 153.

(7) Gordon, M.; Ware, W. R., Eds. *The Exciplex*; Academic Press: New York, 1975.

(8) (a) Asahi, T.; Mataga, N. *J. Phys. Chem.* **1989**, *93*, 6575. (b) Asahi, T.; Mataga, N. *J. Phys. Chem.* **1991**, *95*, 1956. (c) Peters, K. S. In *Advances in Electron-Transfer Chemistry*; JAI Press: New York, 1994; Vol 4, p 27.

(9) (a) Gould, I. R.; Farid, S. *J. Phys. Chem.* **1992**, *96*, 7635. (b) Gould, I. R.; Young, R. H.; Moody, R. E.; Farid, S. *J. Phys. Chem.* **1991**, *95*, 2068.

(10) Gould, I. R.; Young, R. H.; Mueller, L. J.; Farid, S. *J. Am. Chem. Soc.* **1994**, *116*, 8176.

(11) (a) Rehm, D.; Weller, A. *Ber. Bunsenges.* **1969**, *73*, 834. (b) Rehm, D.; Weller, A. *Isr. J. Chem.* **1970**, *8*, 259.

(12) (a) Mataga, N.; Okada, T.; Yamamoto, N. *Chem. Phys. Lett.* **1967**, *1*, 119. (b) Okada, T.; Matsui, H.; Oohari, H.; Matsumoto, H.; Mataga, N. *J. Chem. Phys.* **1968**, *49*, 4717.

(13) (a) Weller, A.; Zachariasse, K. *Chem. Phys. Lett.* **1971**, *10*, 590. (b) Weller, A. *Z. Phys. Chem. N.F.* **1982**, *130*, 129. (c) Baggott, J. E. In *Photoinduced Electron Transfer*; Fox, M. A., Chanon, M., Eds.; Elsevier: New York, 1988; Part B, p 385.

S0002-7863(97)01188-8 CCC: $14.00 © 1997 American Chemical Society

Chart 1

DONORS:

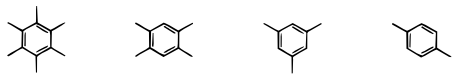

HMB	DUR	MES	XYL	
1.62 V	1.84 V	2.11 V	2.01 V	E°_{ox} (vs. SCE)

ACCEPTORS:

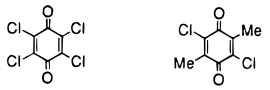

CA	CX	
0.02 V	-0.51 V	E°_{red} (vs. SCE)

their relationship to ground-state electron donor−acceptor (EDA) complexes has been raised.[7,15]

For our studies on the mechanism of bimolecular electron transfer, we used excited quinones as electron acceptors and examined their diffusional interaction with the polymethylbenzene electron donors in Chart 1 by time-resolved (ps/μs) absorption spectroscopy. Chloranil and the related 2,5-dichloroxyloquinone were chosen as transient acceptors for the following reasons: (i) Upon photoexcitation, both quinones form long-lived (μs) excited triplet states[16] which function as powerful one-electron oxidants for a variety of aromatic donors.[17,18] (ii) For chloranil, both exciplex formation[19,20] and electron transfer to the excited state[16−18] have been established. (iii) Both quinones also form EDA complexes with arene donors in the ground state, as established by UV−vis spectroscopy.[21] The use of (a) polymethylbenzenes of various donor strengths[22] and (b) a pair of quinones of different acceptor strength[23] allowed us to vary the driving force for electron transfer over a range of about 10 kcal mol^{-1}. In this study, we show that electron transfers with photoactivated quinones lead to a sequence of spectral transients that span the distinctive time scales from picoseconds to microseconds. Time-resolved spectroscopy enables us to establish in a conclusive way not only their existence, but also their temporal sequence within the electron-transfer manifold. In addition to the time-resolved absorption measurements, the kinetic experiments and the studies of the effects of the solvents (as well as the temperature, the electron-transfer driving force, and the steric hindrance) on the overall electron-transfer dynamics are utilized to characterize (spectroscopically, kinetically, and thermodynamically) the reaction intermediates. A particular focus will be directed to the initial encounter complex of the donor and the acceptor prior to electron transfer.

Results

I. Quinones as Photoactivated Acceptors (Q*). Upon the 10-ns laser excitation at 355 nm of an argon-purged solution of chloranil (**CA**) in acetonitrile, a transient absorption spectrum with double maxima at 380 and 510 nm and a shoulder at 480 mm was observed (Figure 1A) and readily assigned to the triplet state of chloranil (**CA***).[16,24] The absorption bands decayed on the microsecond time scale with lifetimes of $\tau > 10$ μs (depending on the chloranil concentration). A similar transient absorption spectrum (with maxima at 370 and 500 nm and a shoulder at 470 nm, see Figure 1B) was obtained upon laser excitation of 2,5-dichloroxyloquinone (**CX**) under comparable conditions. On the basis of its similarity with the triplet chloranil spectrum and its oxygen-sensitive lifetime, we assigned this transient spectrum to the triplet state of dichloroxyloquinone (**CX***). Similar transient absorption spectra were observed in other solvents such as dichloromethane, chloroform, and carbon tetrachloride upon the laser excitation of **CX** and **CA**. For acetonitrile, the maximum extinction coefficient of the dichloroxyloquinone triplet (**CX***) at 500 nm was $\epsilon_{500} = 5300$ M^{-1} cm^{-1}, and a triplet quantum yield of $\Phi_T = 1.0 \pm 0.05$ was determined by transient actinometry[25] (see Experimental Section). The spectral and kinetic data for the triplet states of chloranil and dichloroxyloquinone are summarized in Table 1.

II. Electron Transfer of Q* with Aromatic Donors. Spectral Observation of the Transient Intermediate. In the presence of high concentrations (0.03−0.3 M) of aromatic donors (ArH), the transient spectra obtained upon 10-ns laser excitation of chloranil or dichloroxyloquinone showed not only the absorption bands of the corresponding triplet states (*vide supra*) but, in addition, broad absorptions were observed in the wavelength region above 700 nm and extending beyond 900 nm. Picosecond time-resolved experiments revealed that the growth of these new absorptions at long wavelengths was not concomitant with the appearance of the absorption bands of Q* at 500 nm. For example, upon the 25-ps (laser) excitation of a solution of **CA** (0.005 M) and mesitylene (0.1 M) in acetonitrile, we observed the slower growth of a broad absorption band at $\lambda > 800$ nm to occur over a time period of about 1 ns (see Figure 2A). In marked contrast, the 500-nm absorption band of **CA*** was observed immediately attendant upon the 25-ps laser excitation.[26] Similar broad absorptions in the wavelength region above 700 nm were observed upon laser excitation of

(14) (a) Kikuchi, K.; Niwa, T.; Takahashi, Y.; Ikeda, H.; Miyashi, T.; Hoshi, M. *Chem. Phys. Lett*. **1990**, *173*, 421. (b) Kikuchi, K.; Takahashi, Y.; Katagiri, T.; Niwa, T.; Hoshi, M.; Miyashi, T. *Chem. Phys. Lett*. **1991**, *180*, 403.

(15) (a) Kobashi, H.; Okada, T.; Mataga, N. *Bull. Chem. Soc. Jpn*. **1986**, *59*, 1975. (b) Kawai, K.; Shirota, Y.; Tsubomura, H.; Mikawa, H. *Bull. Chem. Soc. Jpn*. **1972**, *45*, 77.

(16) (a) For chloranil, see: Gschwind, R.; Haselbach, E. *Helv. Chim. Acta* **1979**, *62*, 941. (b) **CX** and 1,4-benzoquinone have similar reduction potentials. However, the short triplet lifetime (<10 ns)[16c] of benzoquinone precluded its use in this study. (c) Kemp, D. R.; Porter, G. *Proc. R. Soc. London, Ser. A* **1971**, *326*, 117.

(17) (a) Kawai, K.; Shirota, Y.; Tsubomura, H.; Mikawa, H. *Bull. Chem. Soc. Jpn*. **1972**, *45*, 77. (b) Creed, D. In *Organic Photochemistry and Photobiology*; Horspool, W. M., Song, P.-S., Eds; CRC Press: Boca Raton, FL, 1995; p 737. (c) Bockman, T. M.; Kochi, J. K. *J. Chem. Soc., Perkin Trans. 2* **1996**, 1633. (d) Johnston, L. J.; Schepp, N. P. *J. Am. Chem. Soc*. **1993**, *115*, 6564.

(18) Jones, G., II; Haney, W. A. *J. Phys. Chem*. **1986**, *90*, 5410.

(19) (a) Kobashi, H.; Funabashi, M.-A.; Kondo, T.; Morita, T.; Okada, T.; Mataga, N. *Bull. Chem. Soc. Jpn*. **1984**, *57*, 3557. (b) Kobashi, H.; Kondo, T.; Funabashi, M.-A. *Bull. Chem. Soc. Jpn*. **1986**, *59*, 2347. (c) Kobashi, H.; Hiratsuka, K.-I.; Motegi, K. *Bull. Chem. Soc. Jpn*. **1988**, *61*, 298. (d) Levin, P. P.; Tatikolov, A. S.; Kuz'min, V. A. *Bull. Acad. Sci. USSR, Div. Chem. Sci*. **1982**, *31*, 890. (e) Levin, P. P.; Kuz'min, V. A. *Bull. Acad. Sci. USSR, Div. Chem. Sci*. **1986**, *35*, 1303. (f) Levin, P. P.; Kuz'min, V. A. *Russ. Chem. Rev*. **1987**, *56*, 307. (g) Levin, P. P.; Pluzhnikov, P. F.; Kuz'min, V. A. *Chem. Phys*. **1989**, *137*, 331. (h) Levin, P. P.; Raghavan, P. K. N. *Chem. Phys. Lett*. **1991**, *182*, 663.

(20) Tahara, T.; Hamaguchi, H.-O. *J. Phys. Chem*. **1992**, *96*, 8252.

(21) Foster, R. *Organic Charge-Transfer Complexes*; Academic Press: New York, 1969; p 40.

(22) Howell, J. O.; Goncalves, J. M.; Amatore, C.; Klasinc, L.; Wightman, R. M.; Kochi, J. K. *J. Am. Chem. Soc*. **1984**, *106*, 3968.

(23) (a) The reduction potential of chloranil is $E^{\circ}_{red} = 0.02$ V *vs* SCE; see ref 23c,d. (b) The reduction potential of dichloroxyloquinone is $E^{\circ}_{red} = -0.51$ V *vs* SCE in dichloromethane containing 0.1 M TBA$^+$ PF_6^-. (c) Mann, C. K.; Barnes, K. K. *Electrochemical Reactions in Non-Aqueous Systems*; Dekker: New York, 1970. (d) Peover, J. E. *J. Chem. Soc*. **1962**, 4540.

(24) (a) Kemp, D. R.; Porter, G. *J. Chem. Soc. (D)* **1969**, 1029. (b) Porter, G.; Topp, M. R. *Proc. R. Soc*. **1970**, *A315*, 163. (c) Kobashi, H.; Gyoda, H.; Morita, T. *Bull. Chem. Soc. Jpn*. **1977**, *50*, 1731.

(25) Hurley, J. K.; Sinai, N.; Linschitz, H. *Photochem. Photobiol*. **1983**, *38*, 9.

(26) (a) Hubig, S. M.; Bockman, T. M.; Kochi, J. K. *J. Am. Chem. Soc*. **1997**, *119*, 2926. (b) Hilinski, E. F.; Milton, S. V.; Rentzepis, P. M. *J. Am. Chem. Soc*. **1983**, *105*, 5193.

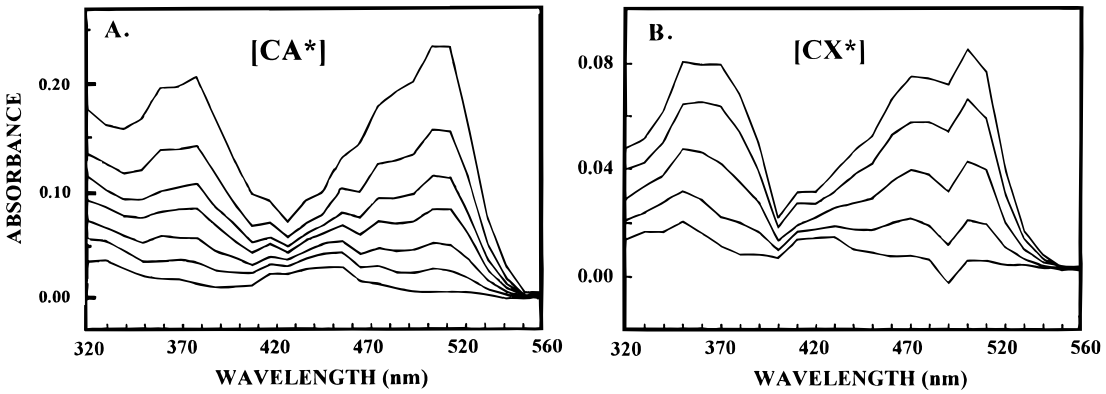

Figure 1. Triplet absorption spectra of (A) chloranil and (B) 2,5-dichloroxyloquinone observed in the time interval of (top-to-bottom) 1.3−15 μs upon the 10-ns laser excitation at 355 nm.

Table 1. Spectral and Kinetic Characterization of the Triplet States of Chloranil (^{3}**CA**) and Dichloroxyloquinone (^{3}**CX**) in Acetonitrile

parameter	^{3}**CA**	^{3}**CX**
$\lambda_{T-T,\ max}$ [nm][a]	510	500
$\epsilon_{T-T,\ max}$ [M^{-1} cm^{-1}][b]	7570[c]	5300
Φ_T[d]	0.98 ± 0.05[c]	1.00 ± 0.05
τ_T [μs][e]	>10	>2

[a] Wavelength maximum of the triplet absorption band. [b] Triplet extinction coefficient. [c] Reference 16. [d] Triplet quantum yield. [e] Triplet lifetime.

CX in the presence of the various aromatic donors in Chart 1. These new infrared (NIR) bands were not only observed in acetonitrile, but also in other less polar solvents such as dichloromethane, chloroform, and carbon tetrachloride. For example in chloroform, the 25-ps laser excitation of **CX** and durene led to new absorption in the NIR region above 700 nm, as shown in Figure 2B. Strikingly, the slow growth of the broad NIR absorption at 70, 570, and 1070 ps occurred under conditions in which the local band of **CX*** centered at 500 nm remained unchanged[27]—as underscored by the enlargements in the insets for both absorption bands. Although the spectral maxima of the near-IR absorptions were beyond our detector limit (see Experimental Section), Figure 3 clearly shows the bathochromic shifts in the absorption onsets to occur in the following order: **CX**/DUR < **CX**/HMB < **CA**/MES < **CA**/XYL. The new absorptions at wavelengths above 700 nm are hereinafter ascribed to the *transient intermediate* (TI) between the excited quinone and the arene donor.

From the rise time of the near-infrared absorption band in Figure 2A, we determined the first-order rate constant for the formation of the transient intermediate from chloranil and mesitylene as $k_{obs} \simeq 1 \times 10^9$ s^{-1}. For a mesitylene concentration of 0.1 M, we calculated the bimolecular rate constant for TI formation to be $k_{TI} \simeq 1 \times 10^{10}$ M^{-1} s^{-1}, which is on the time scale of diffusion-controlled processes. TI formation was also observed on the early nanosecond time scale in **CX** solutions containing durene (Figure 2B), and the diffusion-controlled values for k_{TI} were found to be the same for both quinones and other donors (DUR, HMB, and XYL).

III. The Decay of the Transient Intermediate with the Concomitant Formation of Ion Radicals in Acetonitrile. The absorption spectra described in the previous section decayed rapidly on the nanosecond time scale. For example, the absorption band (above 700 nm) observed upon the 10-ns laser excitation at 355 nm of dichloroxyloquinone/durene in acetonitrile decreased simultaneously with the decay of the absorption band of **CX*** with a first-order rate constant of $k_{dec} = 5.5 \times 10^7$ s^{-1} (see Figure 4), and new narrow absorption bands centered at 330 and 430 nm grew in at the same rate. The new absorptions were readily assigned to the anion-radical of dichloroxyloquinone (**CX**$^{\bullet-}$) by spectral comparison with that generated independently.[28] Subsequently, the 330- and 430-nm absorption bands of the anion radical of dichloroxyloquinone slowly decayed by second-order kinetics on the microsecond time scale.

Similar time-resolved spectra on the nanosecond time scale were obtained upon laser excitation of dichloroxyloquinone in the presence of hexamethylbenzene (0.01 M) in acetonitrile, and upon photoexcitation of chloranil in the presence of either mesitylene or xylene in acetonitrile. In all cases, the initial spectrum upon the 10-ns laser excitation showed the diagnostic absorption band (above 700 nm) of the transient intermediate of the quinone and the arene (ArH). This absorption decayed by first-order kinetics on the nanosecond time scale concomitant with the 500-nm absorption of Q* to generate the spectrum of the quinone anion radical ($Q^{\bullet-}$). In all cases, we assigned the decay of the quinone/arene intermediates to the coproduction of ion radicals ($Q^{\bullet-}$ and $ArH^{\bullet+}$). [The absorption bands of the accompanying cation radicals of the arene donors ($ArH^{\bullet+}$) were not directly monitored owing to their low extinction coefficients and spectral overlap with the strongly absorbing quinone anion radicals.[29]] On the basis of the extinction coefficients of dichloroxyloquinone ($\epsilon_{430} = 6800$ M^{-1} cm^{-1})[28] and chloranil ($\epsilon_{450} = 9700$ M^{-1} cm^{-1}),[30] the ion radical yields of $\Phi_{ion} = 1.0 \pm 0.05$ were determined for various quinone/arene combinations in acetonitrile with benzophenone as the transient actinometer[25] (see Experimental Section).

IV. The Fate of the Transient Intermediate in Solvents of Low Polarity. In the less polar solvents such as dichloromethane, chloroform, or carbon tetrachloride, the decay of

(27) The temporal behavior of **CA*** (centered at 510 nm) decoupled from the slower formation of the NIR band was obscured in acetonitrile by the rapid followup reactions (*i.e.* ion-pair formation, *vide infra*) that occurred on the same time scale.

(28) The **CX**$^{\bullet-}$ anion radical was generated by electron-transfer quenching of **CX*** with 4,4′-dimethylbiphenyl, dibenzofuran, and hexamethylbenzene. The electron-transfer quenching experiment with 4,4′-dimethylbiphenyl, which yielded the biphenyl cation radical[29] and the dichloroxyloquinone anion radical, was also used to determine the extinction coefficient of **CX**$^{\bullet-}$ at 430 nm to be $\epsilon_{430} = 6800 \pm 100$ M^{-1} cm^{-1}.

(29) (a) It is noteworthy that the absorption spectra of biphenyl and naphthalene cation radicals were sufficiently red-shifted[29b] to allow simultaneous observation with the chloranil anion radical in a roughly 1:1 molar ratio. In these cases, however, the NIR absorption of the encounter complex was not sufficiently resolved to allow quantitative spectral evaluation. (b) Shida, T. *Electronic Absorption Spectra of Radical Ions*; Elsevier: Amsterdam, 1988.

(30) The absorption maximum of chloranil anion radical in acetonitrile is centered at 450 nm. See: André, J. J.; Weill, G. *Mol. Phys.* **1968**, *15*, 97.

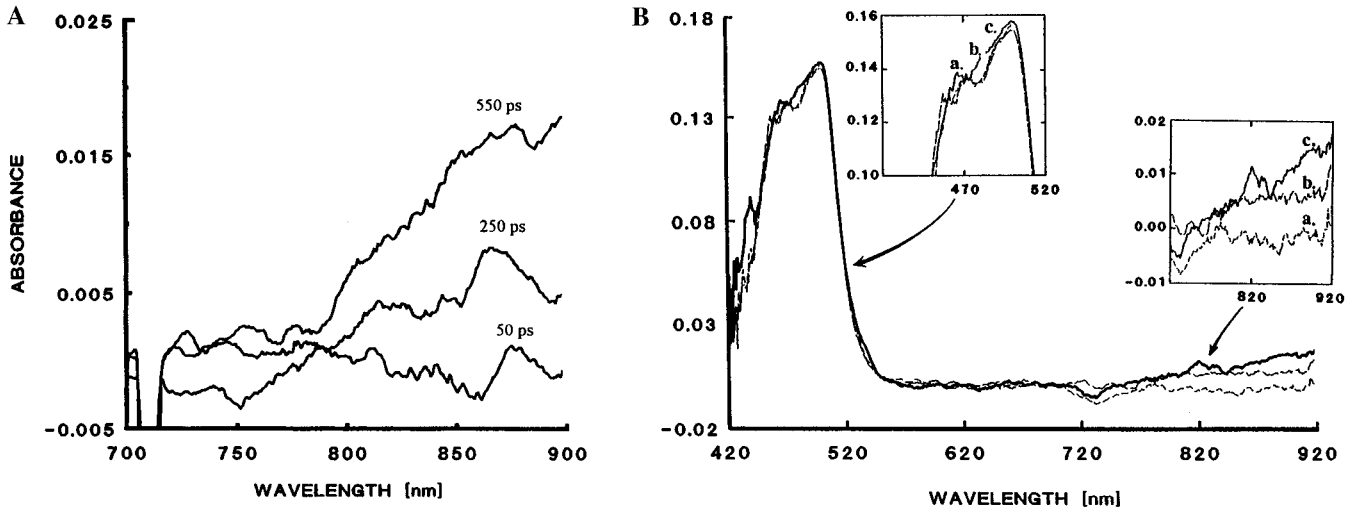

Figure 2. Temporal evolution of the near-IR band at $\lambda > 700$ nm from (A) 0.002 M chloranil and 0.1 M mesitylene in acetonitrile and (B) 0.002 M **CX** and 0.1 M durene in chloroform following the application of the 25-ps laser pulse at 355 nm. The insets (×5) in part B establish the invariance of the local band of **CX*** at 500 nm during the slower growth period of the CT absorption at $\lambda > 700$ nm in the time interval among (a) 70 ps, (b) 570 ps, and (c) 1.07 ns.

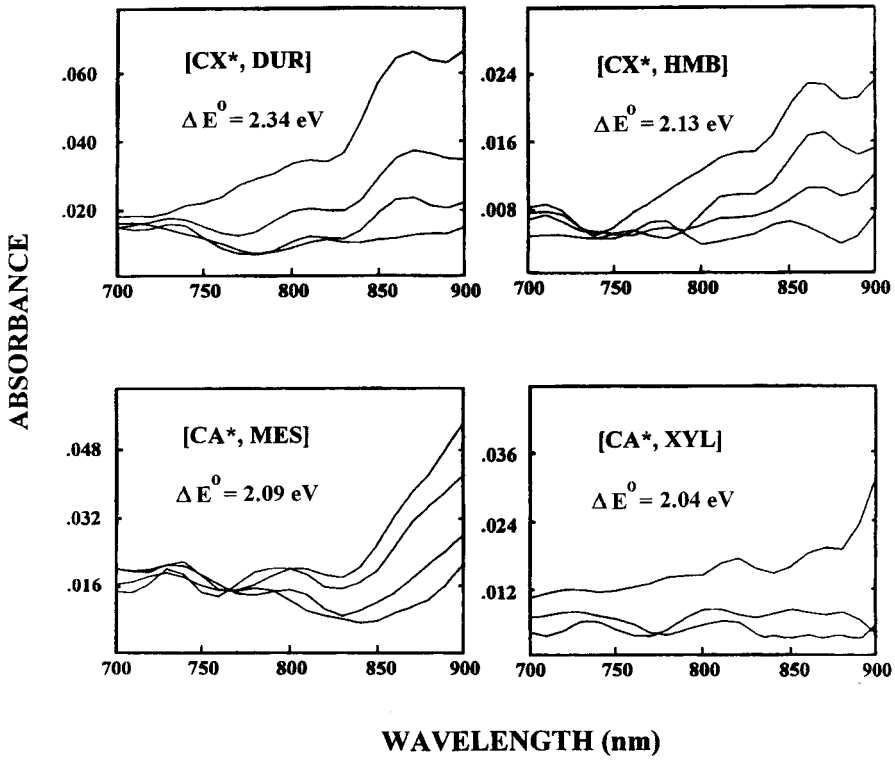

Figure 3. Progressive bathochromic shift of the near-IR absorptions with decreasing energy gap ($\Delta E°$) between the oxidation potential of the aromatic donor and the reduction potential of the quinone acceptor in chloroform.

the transient intermediates did not result in the formation of the ion-radical pair $Q^{\bullet -}$ and $ArH^{\bullet +}$. Instead, the protonated quinone anion radical (Q-H$^{\bullet}$)[18] was the species observed after the decay of the transient intermediate. For example, immediately upon 10-ns laser excitation of dichloroxyloquinone/durene in chloroform, the spectrum of the transient intermediate was observed with an absorption maximum at 500 nm and a broad tail absorption extending beyond 900 nm (Figure 5). The TI absorption decayed completely to baseline within 400 ns ($k_{dec} = 1.6 \times 10^7$ s^{-1}) and ultimately led to a new spectrum with a very narrow absorption band at 420 nm (see Figure 5). The 420-nm absorption was readily assigned to the protonated form of the dichloroxyloquinone anion radical (**CX-H$^{\bullet}$**) by spectral comparison with that of the chloranil analogue (*vide infra*).

A. Solvent Variation. Similar transient spectra were obtained upon the quenching of **CX*** with hexamethylbenzene and in other solvents of low polarity such as dichloromethane or carbon tetrachloride. In the case of chloranil, the protonated chloranil anion radical (**CA-H$^{\bullet}$** or hydrochloranil) was observed.[18] Hydrochloranil yields could be estimated on the basis of its extinction coefficient at 435 nm ($\epsilon_{435} = 7700$ M^{-1} cm^{-1}).[31] For example, the quenching of **CA*** by mesitylene led to the **CA-H$^{\bullet}$** in a yield of $\Phi = 0.7 \pm 0.1$, which was invariant in dichloromethane, chloroform, and carbon tetrachloride. Similarly, the yields of protonated anion radicals generated from

(31) Wong, S. K.; Fabes, L.; Green, W. J.; Wan, J. K. S. *J. Chem. Soc., Faraday Trans. 1* **1972**, *68*, 2211.

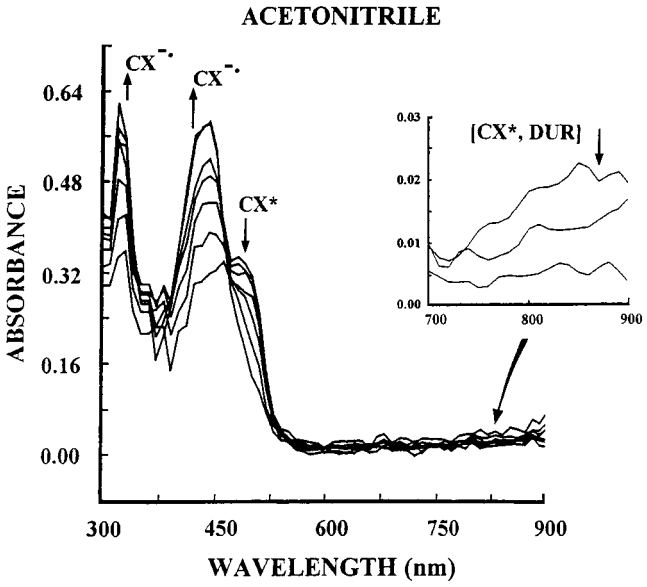

Figure 4. Transient absorption spectra from 0.002 M **CX** and 0.04 M DUR in acetonitrile following the 10-ns laser excitation at 355 nm. The absorption bands of **CX*** with $\lambda_{max} = 500$ nm and [**CX***, DUR] at $\lambda > 700$ nm (see inset) decayed with the same rate constant ($k = 5.4 \times 10^7$ s^{-1}) as the first-order appearance of **CX**$^{\bullet-}$ at $\lambda_{max} = 330$ and 430 nm.

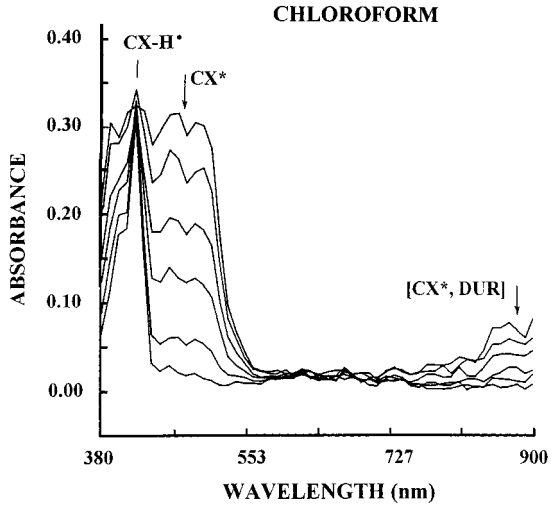

Figure 5. Transient absorption spectra from 0.002 M **CX** and 0.3 M DUR in chloroform following the 10-ns laser excitation at 355 nm to show the absorption bands of **CX*** and [**CX***/DUR] decaying at identical rates ($k = 1.4 \times 10^7$ s^{-1}). After an interval of 200 ns, only the narrow absorption band of the protonated anion radical (**CX-H**$^{\bullet}$ with $\lambda_{max} = 420$ nm) is observed.

dichloroxyloquinone did not vary significantly in dichloromethane, chloroform, and carbon tetrachloride ($\Phi = 0.5-0.7$).

B. Salt Effects. Upon the photoexcitation of dichloroxyloquinone in the presence of durene dissolved in chloroform containing 0.1 M tetra-*n*-butylammonium hexafluorophosphate ($TBA^+PF_6^-$), we initially observed the formation of the transient intermediate with its characteristic near-IR absorbance beyond 700 nm, as previously observed in the absence of added salt. However, the decay of the transient intermediate in the presence of added salt did not lead to protonated quinone anion radicals (as observed in the absence of $TBA^+PF_6^-$), but the quinone anion radical itself (**CX**$^{\bullet-}$) was detected with yields of $\Phi_{ion} \cong 0.7$. A similar transformation from the transient intermediate to the ion radical could be achieved with other donor/acceptor pairs in chloroform by the addition of salt, and ion radical yields of 0.7 and 0.3 were obtained for the dichloroxyloquinone/hexamethylbenzene and chloranil/mesitylene pairs, respectively.

V. Evaluation of the Electron-Transfer Kinetics of Q*. For the kinetic studies, the spectral decays in Figures 4 and 5 were monitored on the nanosecond/microsecond time scale as a function of the concentration of aromatic donor, solvent, temperature, and added salt as follows.

1. Dependence on Donor Concentration. 2,5-Dichloroxyloquinone (0.002 M) was photoexcited in chloroform at 355 nm with a 10-ns laser pulse, and the first-order decay (k_{obs}) of the transient absorbance at 500 nm was monitored on the nanosecond/microsecond time scale as a function of added durene. For concentrations up to 0.005 M, the kinetics plots in Figure 6A revealed a more or less linear dependence of k_{obs} on the durene concentration. However, at higher concentrations (>0.005 M), the decay rates did not increase linearly with increasing durene concentration, and a limiting plateau value of $k_{max} = 1.6 \times 10^7$ s^{-1} was obtained for concentrations >0.2 M (see the triangles in Figure 6A). Similar (curved) plots were also obtained in acetonitrile, dichloromethane, and carbon tetrachloride (see Figure 6A). Most notably, the degree of curvature and the absolute value of k_{max} for the plateau varied dramatically with the solvent.

The limiting values of k_{obs} shown in Figure 6A at high donor concentrations were diagnostic of a preequilibrium intermediate[32] between the excited quinone and the aromatic donor. As such, the asymptotic behavior could be readily linearized in a double-reciprocal presentation, from which the formation constant K_{TI} of the transient intermediate between quinone and donor and its intrinsic decay constant (k) could be readily extracted, *i.e.*

$$\frac{1}{k_{obs}} = \frac{1}{k} + \frac{1}{K_{TI}k[D]} \qquad (2)$$

[Note that the slow natural decay of Q* (k_0 in the absence of donor)[16] was irrelevant, since $k_0 \ll k$.] The values for K_{TI} and k, as evaluated from the double-reciprocal plots such as those in Figure 6B, are listed in Table 2 for various quinone/arene combinations. Since the spectral decays clearly led to ion-

(32) For a general kinetics description, see: (a) Espenson, J. D. *Chemical Kinetics and Reaction mechanisms*, 2nd ed.; McGraw-Hill: New York, 1995; p 89f. (b) Connors, K. A. *Chemical Kinetics: The Study of Reaction Rates in Solution*; VCH: New York, 1990; p 101. (c) See also: Kobashi, H.; Okada, T.; Mataga, N. in ref 15a. (d) The ground-state EDA complex in Table 4 cannot contribute significantly to the curvature in Figure 6A since the formation constant $K_{EDA} < 7$ M^{-1} indicated that its concentration was diminishingly small.

(33) Since the Coulombic work terms and solvation energies from all quinone/arene combinations are taken to be invariant (and omitted from eq 4), the simple approximation for ΔG_{ET} underscores the dominant driving-force dependence on the electrode potentials.

(34) Iverson, D. J.; Hunter, G.; Blount, J. F.; Damewood, J. R., Jr.; Mislow, K. *J. Am. Chem. Soc.* **1981**, *103*, 6073.

(35) Hubig, S. M.; Rathore, R.; Kochi, J. K. To be submitted for publication.

(36) Benesi, H. A.; Hildebrand, J. H. *J. Am. Chem. Soc.* **1949**, *71*, 2703.

(37) (a) Mulliken, R. S. *J. Am. Chem. Soc.* **1950**, *72*, 600. (b) Mulliken, R. S. *J. Am. Chem. Soc.* **1952**, *74*, 811. (c) Mulliken, R. S. *J. Phys. Chem.* **1952**, *56*, 801. (d) Mulliken, R. S.; Person, W. M. *Molecular Complexes*; Wiley: New York, 1969. (e) In Mulliken theory, the charge-transfer absorption band varies as $hc/\lambda_{CT} = IP - EA - \omega$, where IP is the ionization potential of the donor, EA is the electron affinity of the acceptor, and ω is the electrostatic work term of the ion pair [D$^{\bullet+}$,A$^{\bullet-}$]. This relationship can be approximated as $hc/\lambda_{CT} = \Delta E +$ constant, where ΔE is the energy gap (in solution) for structurally related D/A pairs. Mulliken theory also predicts K_{EDA} to increase with increasing donor and acceptor strengths.

(38) A detailed analysis of these steric effects has been presented separately. See: Rathore, R.; Lindeman, S. V.; Kochi, J. K. *J. Am. Chem. Soc.* **1997**, *119*, 9393.

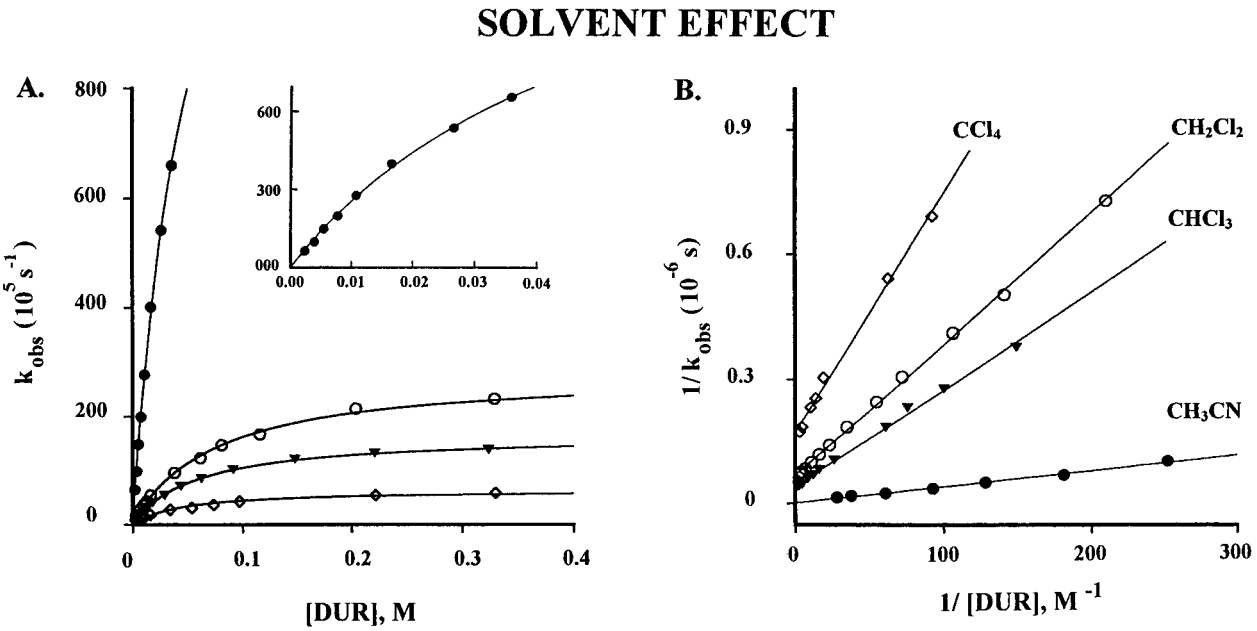

Figure 6. (A) Asymptotic behavior in various solvents of the rate constant (k_{obs}) for electron transfer from durene to **CX*** with increasing donor concentration and (B) its double-reciprocal evaluation according to eq 2. The solid lines in part A represent computer simulations of the data points with the values of K_{TI} and k from Table 2. The inset in part A magnifies (×10) the acetonitrile data to establish the nonlinear trend.

Table 2. Kinetic Data for Electron Transfer from Arene Donors to Photoactivated Quinones

quinone/arene combination[a]	kinetic parameters[b]	solvents			
		CH_3CN	CH_2Cl_2	$CHCl_3$	CCl_4
CX/DUR	k_2 [10^8 M^{-1} s^{-1}]	25.6 (25.5)	3.0 (3.8)	2.3[d] (2.9)	1.1 (1.4)
	K_{TI} [M^{-1}]	15	14	18[e]	24
	k_{ET} [10^7 s^{-1}]	17	2.7	1.6[f]	0.6
CX/HMB[g]	k_2 [10^8 M^{-1} s^{-1}]	51.4	55 (73)	23 (37)	23 (36)
	K_{TI} [M^{-1}]	*c*	67	71	202
	k_{ET} [10^7 s^{-1}]	*c*	11	5.2	1.8
CA/MES	k_2 [10^8 M^{-1} s^{-1}]	39	12 (11)	6.7 (11.3)	2.5 (3.9)
	K_{TI} [M^{-1}]	*c*	30	54	49
	k_{ET} [10^7 s^{-1}]	*c*	3.6	2.1	0.8
CA/XYL	k_2 [10^8 M^{-1} s^{-1}]	54	12 (8.0)	6.6 (6.8)	1.8 (2.9)
	K_{TI} [M^{-1}]	*c*	10	19	21
	k_{ET} [10^7 s^{-1}]	*c*	8.0	3.6	1.4

[a] **CX** = 2,5-dichloroxyloquinone, **CA** = chloranil, HMB = hexamethylbenzene, DUR = durene, MES = mesitylene, XYL = *p*-xylene. [b] See text. The k_2 values are extracted from the initial slope of the kinetics plots. The values in parentheses are the calculated rate constants (see text). [c] Not determined owing to insufficient curvature of kinetics plots (see text). [d] In the presence of salt: 2.1 (3.6) × 10^8 M^{-1} s^{-1}. [e] In the presence of salt: 15 M^{-1}. [f] In the presence of salt: 2.4 × 10^7 s^{-1}. [g] The k_2 values for the hindered analogue hexaethylbenzene are 9.7 × 10^8, 1.6 × 10^8, 0.4 × 10^8, and 0.04 × 10^8 M^{-1} s^{-1} in acetonitrile, dichloromethane, chloroform, and carbon tetrachloride, respectively.

radical pairs (compare Figure 4), the kinetic process must be derived from electron transfer, *i.e.* $k = k_{ET}$.

For low donor concentrations of [D] < 0.005 M, a linear correlation between the rate constant (k_{obs}) for first-order decay and the donor concentration ([D]) was found, which also allowed us to determine the bimolecular rate constant (k_2) from the initial slope of the kinetics plots. For this concentration range, eq 2 was simplified to a linear correlation between k_{obs} and [D] to reveal the relationship between k_2, K_{TI}, and k_{ET} as presented in eq 3:

$$k_{obs} = K_{TI}k_{ET}[D] = k_2[D] \qquad (3)$$

According to eq 3, the bimolecular rate constant (k_2) could be determined either empirically as the slope of the initial (linear) part of the kinetics plots or arithmetically as the product of K_{TI} and k_{ET}, both being extracted from the double-reciprocal analysis (eq 2) of the entire (curved) plots. Table 2 summarizes the values of k_2, K_{TI}, and k_{ET} for four combinations of quinones and arene donors in four solvents. In acetonitrile, significant curvature of the k_{obs}/[D] diagrams was only obtained in the case of the dichloroxyloquinone/durene system, which allowed us to extract values of K_{TI} and k_{ET} according to eq 2. The other quinone/donor combinations did not exhibit sufficient curvature in the k_{obs} *vs* [D] plots to obtain reliable values of K_{TI} and k_{ET} in acetonitrile. The lack of sufficient curvature in these cases arose from the plateau values of k_{obs} which severely exceeded the time resolution of the 10-ns laser pulse ($k_{max} \gg 10^8$ s^{-1}).

2. Solvent and Driving-Force Dependence of the Kinetic Parameters. As shown in Table 2, each kinetic parameter (*viz*, k_2, K_{TI}, and k_{ET}) exhibited its particular solvent dependence. For example, the K_{TI} values increased by a factor of 2−3 with decreasing solvent polarity. On the other hand, the solvent dependence of k_{ET} in Table 2 followed the opposite trend as compared to that of K_{TI}. Thus with increasing solvent polarity, the values of k_{ET} showed significant increases. This effect was best illustrated with the dichloroxyloquinone/durene pair for which we could compare k_{ET} data in all four solvents. Thus, k_{ET} increased by a factor of 28 going from carbon tetrachloride to acetonitrile. The solvent effect on k_{ET} was very similar for all four quinone/donor combinations in Table 2. The k_2 values in Table 2 followed the same solvent trend as described for k_{ET}. The latter was not surprising if one considers the fact that k_2 represented the product of k_{ET} and K_{TI} (see eq 3). In fact, the empirical data for k_2 in Table 2, which were obtained from the initial slopes of the plots, matched the computed values of $K_{TI}k_{ET}$ (given in parentheses) fairly well.

To analyze the driving-force dependence of k_{ET}, the free-energy change (ΔG_{ET}) on proceeding from the transient intermediate to the ion radical was evaluated for each donor−acceptor pair in Table 2. As a reasonable approximation for

Table 3. Temperature Dependence of the Kinetic Parameters for the Electron Transfer from Durene to Photoactivated Dichloroxyloquinone in Acetonitrile

temp (K)	k_2[a] (10^8 M^{-1} s^{-1})	K_{TI}[b] (M^{-1})	k_{ET}[c] (10^8 s^{-1})
295	25.6	15	1.7
277	26.2	65	0.6
253	26.0	90	0.5

[a] Bimolecular rate constant determined from the slope of the initial (linear) portion of the kinetics plot. [b] TI formation constant. [c] First-order rate constants of the decay of the transient intermediate by electron transfer.

ΔG_{ET}, we took the sum of the triplet energy (E_T = 2.13 eV[39]) of the corresponding quinone and the potential difference between the oxidation potential (E°_{ox}) of the arene donor and the reduction potential (E°_{red}) of the quinone acceptor,[33] *i.e.*

$$-\Delta G_{ET} = E_T - E^\circ_{ox} + E^\circ_{red} + \text{constant} \qquad (4)$$

Although there were only four data points per solvent, a consistent pattern was noticeable in that k_{ET} increased by a factor of 2−3 in going from the most endothermic pair (*viz*, dichloroxyloquinone/durene: ΔG_{ET} = +0.21 eV) to the most exothermic pair (*viz*, chloranil/xylene: ΔG_{ET} = −0.09 eV) in Table 2. We also noted a peculiar driving-force dependence of K_{TI}. Thus, the largest TI formation constants were found for the transient intermediates derived from either chloranil/mesitylene or dichloroxyloquinone/hexamethylbenzene (see Table 2). Interestingly, these were the two quinone/arene combinations for which ΔG_{ET} was equal or very close to zero (see Discussion).

3. Temperature Dependence of the Electron-Transfer Kinetics. Electron-transfer quenching of photoexcited dichloroxyloquinone by durene in acetonitrile was monitored at 4 and −20 °C, and the data were compared with those obtained at room temperature. The k_{obs} *vs* [D] plots at the lower temperatures were also curved in a manner similar to that obtained at room temperature. The kinetic parameters K_{TI} and k_{ET} were extracted from the double-reciprocal fit of the kinetic data according to eq 2. As shown in Table 3, the value of K_{TI} increased and that of k_{ET} decreased significantly at the lower temperatures. However, the bimolecular rate constant [k_2 as determined from the slope of the initial (linear) portion of the plot] showed no variation over the entire temperature range of 40 °C. The temperature dependence of the formation constants (K_{TI}) was evaluated from the van't Hoff relationship, and a formation enthalpy of ΔH_{TI} = −5.6 kcal mol^{-1} was extracted from the plot of ln K_{TI} *vs* the reciprocal temperature. The free-energy change at the medium temperature of 277 K was $\Delta G_{TI} = -RT \ln K_{TI}$ = −2.3 kcal mol^{-1}, and the entropy change of TI formation was calculated to be ΔS_{TI} = −12 cal mol^{-1} K^{-1} from the Gibbs equation.

4. Effects of Added Salt on Electron-Transfer Kinetics. As described above, the addition of an inert salt to solvents of low polarity led to quinone anion radicals ($Q^{\bullet-}$) as opposed to protonated anion radicals (Q-H$^\bullet$) in the absence of salt. However, *the kinetics were remarkably unaffected by the presence of salt*. For example, the addition of 0.1 M tetra-*n*-butylammonium hexafluorophosphate to a solution of dichloroxyloquinone and durene in chloroform raised the plateau value of k_{obs} only slightly, and the formation constant K_{TI} was not affected at all by the added salt. In Figure 7, the corresponding acetonitrile data were replotted to demonstrate the remarkably different effects of solvent polarity and addition of salt on the electron-transfer kinetics.

(39) Murov, S. L.; Carmichael, I.; Hug, G. L. *Handbook of Photochemistry*; Dekker: New York, 1993.

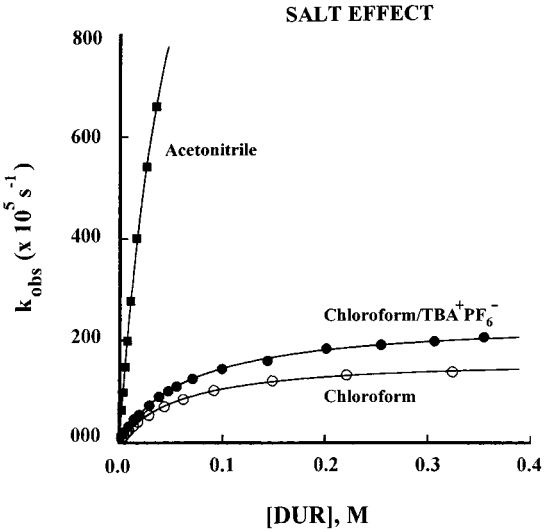

Figure 7. Salt effect on the rate constants (k_{obs}) for electron transfer from durene to **CX*** in (●) chloroform containing 0.1 M $TBA^+PF_6^-$ relative to that in either (○) chloroform alone or (■) acetonitrile alone. The solid lines represent the computer simulations of the data points according to eq 2 with the values of K_{TI} and k from Table 2.

5. Steric Effects on Electron-Transfer Kinetics. To study the structural effects of the donor on the electron-transfer kinetics, we compared the k_{obs} *vs* [D] plots and the time-resolved spectra of photoexcited quinones with hindered and nonhindered polymethylbenzenes of similar oxidation potentials. Whereas the dichloroxyloquinone/durene data showed curved kinetics plots (see Figure 6A), the correlation between k_{obs} and the donor concentration in the case of the highly hindered hexaethylbenzene[34] or octamethyloctahydroanthracene[35] remained remarkably linear even to very high donor concentrations. Moreover, the transient absorption spectra exhibited only the absorption bands of **CX*,** and no transient (near IR) absorptions beyond 700 nm were detected. Similar results were obtained in the comparison of other pairs of hindered and nonhindered aromatic donors. In all experiments with the sterically hindered donors, we did not detect any of the diagnostic signs for the formation of the transient intermediate, as deduced from the absence of transient absorption bands at long wavelengths and the lack of curvature in the kinetics plots. Thus, neither spectroscopic nor kinetic evidence was observed for the formation of the transient intermediate from hindered donors prior to electron transfer.

VI. Ground-State Formation of Electron Donor−Acceptor (EDA) Complexes of Quinones with Arene Donors. Chloranil as well as dichloroxyloquinone both formed (ground-state) electron donor−acceptor complexes[21] with the various polymethylbenzenes in Chart 1, as revealed by the typical charge-transfer absorption bands observed immediately upon mixing solutions of quinones and arenes. It is particularly important to emphasize that the spectral changes in Figure 8 showed that the intensity of the CT absorption band at λ_{CT} = 522 nm increased with donor concentrations under conditions in which the local band of chloranil at λ_{max} = 374 nm was singularly invariant. In other words, the ground-state EDA complexes consisted of the superposition of two absorption bands—one from the quinone itself and one from the Q/D charge transfer—as originally predicted by Mulliken.[37] Table 4 lists the spectral maxima (λ_{CT}) of the charge-transfer absorption bands and the formation constants (K_{EDA}) for the electron donor−acceptor complexes of various quinone/arene combinations in four solvents determined by the Benesi−Hildebrand method[36] (see Experimental Section). For all donor−acceptor combinations, a significant decreasing trend of the formation

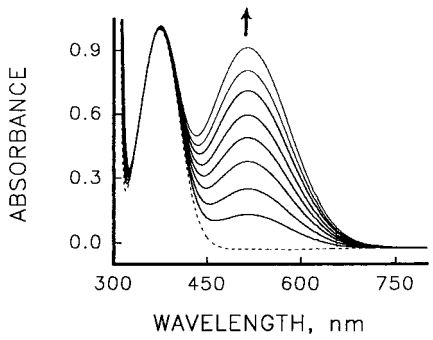

Figure 8. Charge-transfer absorption band at $\lambda_{max} = 522$ nm of the EDA complex of 0.004 M chloranil with increasing concentrations (10−50 mM) of hexamethylbenzene in dichloromethane from ref 38. (The dashed curve is for 0.004 M chloranil alone.)

Table 4: Formation Constants (K_{EDA}), Products $K_{EDA}\epsilon_{CT}$, and the Charge-Transfer Absorption Maxima (λ_{CT}) of Various Electron Donor−Acceptor (EDA) Complexes of Quinones and (Poly)methylbenzenes in Different Solvents[a]

arene/quinone combination[b] (λ_{CT}, nm)	EDA complex parameters[c]	solvent			
		CH_3CN	CH_2Cl_2	$CHCl_3$	CCl_4
CA/HMB (522)	K_{EDA}	0.8	2.8	2.4	6.9
	$K_{EDA}\epsilon_{CT}$	5300	7700	6100	18000
CA/DUR (476)	K_{EDA}	0.6	1.3	1.3	3.9
	$K_{EDA}\epsilon_{CT}$	1200	2200	2300	5000
CA/MES (432)	K_{EDA}	0.3	0.8	0.7	1.9
	$K_{EDA}\epsilon_{CT}$	530	1200	1200	2500
CA/XYL (470)	K_{EDA}	0.5	0.5	d	d
	$K_{EDA}\epsilon_{CT}$	350	460	d	d
CX/HMB (476)	K_{EDA}	0.3	0.5	0.6	1.7
	$K_{EDA}\epsilon_{CT}$	350	460	490	1400
CA/HEB (*e*)	K_{EDA}	0	<0.008	d	d
	$K_{EDA}\epsilon_{CT}$	0	<10	d	d

[a] The values of K_{EDA} and $K_{EDA}\epsilon_{CT}$ were extracted from Benesi−Hildebrand plots, see Experimental Section. [b] HMB = hexamethylbenzene, HEB = hexaethylbenzene, DUR = durene, MES = mesitylene, XYL = xylene, **CA** = chloranil, **CX** = 2,5-dichloroxyloquinone. [c] K_{EDA} = formation constant of the EDA complex in M^{-1}. For the product $K_{EDA}\epsilon_{CT}$, see Experimental Section. [d] Not determined. [e] No new absorption band observed.

constants K_{EDA} was noted with increasing solvent polarity. We also found the strongest complex to be formed between chloranil and hexamethylbenzene, in accord with the dependence of K_{EDA} on the oxidation and reduction potentials of the electron donor and acceptor moieties.[37]

To study structural effects on the formation of EDA complexes, we compared the formation of the ground-state complexes from aromatic donors of similar oxidation potentials, but different steric requirements. For example, hexamethylbenzene and hexaethylbenzene have almost identical oxidation potentials.[22] However, hexamethylbenzene readily formed the various EDA complexes with aromatic acceptors in Table 4, whereas hexaethylbenzene showed no charge-transfer absorption when mixed with chloranil in dichloromethane, even at concentrations close to saturation (1.8 M). Similar steric effects were observed when other pairs of hindered and nonhindered donors were compared.[38]

Discussion

The use of quinones (Q) and aromatic donors (ArH) in Chart 1 allows the temporal course of electron transfer to yield $Q^{\bullet-}$ and $ArH^{\bullet+}$ in eq 1 to be precisely monitored and the sequence of reactive intermediates to be directly observed step by step:

I. Spontaneous Generation of the Electron Acceptor Q*. The application of a 25-ps laser pulse to a quinone (in solution) leads to its efficient excitation to the triplet state Q* with a sizable energy of $E_T \simeq 50$ kcal mol^{-1}.[39] For chloranil and a series of related quinones, Q* is spontaneously generated with unit efficiency,[16] owing to ultrafast intersystem crossing ($k_{ISC} \simeq 10^{11}$ s^{-1}) from the singlet manifold.[26] In other words, Q* is quantitatively formed as a discrete electron acceptor within 50 ps, which allows sufficient time resolution for the fast electron-transfer kinetics to be measured via the temporal evolution of its characteristic absorption spectrum (Figure 1), as follows.

II. Direct Observation and Characterization of the Encounter Complex. The transient absorption spectrum of Q* is strongly affected by the presence of aromatic donors (ArH)—rapidly leading to broad unstructured absorptions of the transient intermediate in the near-infrared (wavelength) region beyond 700 nm shown in Figure 3. Most notably, the bathochromic shifts of the near-IR bands that follow the trend in ΔG_{ET} (as defined in eq 4) point to the charge-transfer (CT) character of the new electronic transition, in accord with Mulliken theory.[37] Indeed, similar NIR absorptions were previously ascribed to exciplexes and spectrally assigned to charge-transfer transitions by Tsubomura, Mataga, and co-workers,[15] and confirmed by time-resolved resonance Raman spectroscopy.[20] In other words, the transient intermediate (TI) identified in this study is identical to these types of exciplexes, and both are best defined in this context as intermolecular complexes of excited quinones with aromatic donors which exhibit spectrally observable charge-transfer character. Accordingly for the purpose of a clear definition,[40] we refer hereinafter to the transient intermediate as the encounter complex (EC) derived from the excited quinone and the aromatic donor, *i.e.*

$$Q^* + ArH \xrightarrow{k_{EC}} \underset{\text{encounter complex}}{[Q^*, ArH]} \qquad (5)$$

As such, k_{EC} for the formation of the encounter complex in eq 5 coincides with the experimentally measured value of $k_{TI} \simeq 1 \times 10^{10}$ M^{-1} s^{-1} for the diffusional rate constant of the transient intermediate from **CA*** and mesitylene (*vide supra*). Most importantly, the absorption spectrum which is assigned to this encounter complex with its near-IR band at $\lambda_{CT} > 800$ nm includes the local absorption band of Q* in the visible region (~500 nm), as established in Figures 2B, 4, and 5. Such spectral features are highly reminiscent of those present in the ground-state EDA complex (see Figure 8). Indeed, the striking spectral comparison of the encounter complex in Figures 2B and 4 with the ground-state EDA complex in Figure 8 demonstrates that the local bands of both quinones (Q* and Q) remain essentially unperturbed by complex formation. Moreover, the spectrum of the encounter complex (consisting of the local quinone and the NIR CT band) is clearly distinguished from the spectrum of the corresponding ion-radical pairs (consisting of the composite absorptions of $Q^{\bullet-}$ and $D^{\bullet+}$ in Figure 4). Most notably, the fast diffusion-controlled formation of the encounter complex is independent of added salt to also distinguish it from the appearance of the ion-radical pair (in chloroform).

III. Charge-Transfer Character of the (Excited-State) Encounter Complex in Comparison with the Electron

(40) The term "exciplex" is frequently used in a wider, but rather ambiguous, way to include both charge-transfer complexes in the excited state (as defined here) as well as ion-radical pairs.[19,20] Since we can clearly distinguish excited CT complexes from contact ion pairs spectroscopically, we prefer *encounter complex* to establish the more general connection of this work to other (adiabatic) electron-transfer processes. For further definitions of encounter complexes, exciplexes, collision complexes, and ion-radical pairs, see also: Kavarnos, G. J.; Turro, N. J. *Chem. Rev.* **1986**, *86*, 401.

Chart 2. Solvent Trends in K_{EDA} and K_{EC}[42]

solvent	(polarity) kcal mol^{-1}	K_{EDA}, M^{-1}	K_{EC}, M^{-1}
CH_3CN	(46)	0.3	<15
CH_2Cl_2	(41)	0.5	67
$CHCl_3$	(30)	0.6	71
CCl_4	(32)	1.7	202

Donor−Acceptor (Ground-State) Complex. The charge-transfer absorption of the encounter complex is far red-shifted beyond $\lambda_{CT}(EC) > 900$ nm,[41] as compared to the CT absorption in the corresponding ground-state EDA complex with $\lambda_{CT}(EDA) \simeq 480$ nm in Table 4. Furthermore, the formation constants of the encounter complex K_{EC} ($=K_{TI}$) in Table 2 are several orders of magnitude larger than the corresponding values K_{EDA} in Table 4. Such differences between the excited-state and ground-state charge-transfer interactions derive naturally from Mulliken theory,[37] if one considers that quinones are much stronger electron acceptors in the excited state (Q*) as compared to the ground state (Q). Indeed, the smaller gap between the donor and acceptor potentials in [Q*, ArH], relative to that in [Q, ArH] as evaluated by the quinone triplet energy of roughly 50 kcal mol^{-1},[39] predicts a corresponding red shift in the CT absorption band to longer wavelength and a concomitant enhancement in the formation constant of the excited-state complex.[15] The further confirmation of the charge-transfer character of these absorptions is shown in Figure 3 by the progressive bathochromic shift of the NIR absorptions with decreasing energy gap ($\Delta E°$) between the oxidation potential of the aromatic donor and the reduction potential of the quinone acceptor according to the expectations of Mulliken theory.[37e] Accordingly, let us consider other ways in which the excited-state and ground-state complexes can be compared.

A. Solvent Dependence of the Formation Constants. The less polar solvents like carbon tetrachloride favor the formation of both the encounter complex (EC) as well as the EDA complex, as shown by the parallel trends in K_{EC} and K_{EDA} in Chart 2.[42] Since the solvent dependence for complex formation is a measure of the difference between the solvation energy of the donor−acceptor complex and of its individual components, the sharply increased trend of K_{EC} above can be taken as a reflection of the more charge-polarized character of the (excited-state) encounter complex relative to K_{EDA} of the ground-state complex. In addition, a solvent of high donicity such as acetonitrile competes with the aromatic donor in complex formation, and leads to lower values of both K_{EC} and K_{EDA}.[43]

Chart 3. Driving-Force Dependence of K_{EC} and K_{EDA}[44]

	ground-state		excited-state	
Q/ArH	ΔG_{gs}, eV	K_{EDA}, M^{-1}	ΔG_{es}, eV	K_{EC}, M^{-1}
CA/HMB	+1.60	2.8	−0.53	<5
CA/DUR	+1.81	1.3	−0.32	<5
CA/XYL	+2.04	0.5	−0.09	10
CA/MES	+2.09	0.8	−0.04	30
CX/HMB	+2.13	0.5	0	67
CX/DUR	+2.34	0.3	+0.21	14

B. Energy-Gap Dependence of the Formation Constant. The charge-transfer character of the (excited-state) encounter complex vis-à-vis the ground-state EDA complex is also manifested in the comparative driving-force dependence of K_{EC} and K_{EDA} summarized in Chart 3.[44] Typically, Mulliken describes weak charge-transfer complexes as the following: $\Psi_N(AD) = a\psi_0(A,D) + b\psi_1(A^- D^+) + ...$, where ψ_0 represents the "no bond" function and ψ_1 is the dative (ion pair) or charge-transfer contribution; and thus the charge-transfer stabilization increases in measure with the ratio of b/a.[37] In the ground-state EDA complex of quinone and arene, the charge-transfer contribution of $\sim b/a$ is diminishingly small, and it is reflected in rather limited values of K_{EDA} that decrease with ΔG_{gs} in Chart 3. By comparison, the larger magnitudes of K_{EC} in the excited-state encounter complex derive from the significantly lower values of ΔG_{es} in Chart 3 that arise from quinone promotion to Q* by $E_T \simeq 50$ kcal mol^{-1}. The latter results in a closer matching of the energy levels of the neutral ("local" excited) state with the ion-pair (charge-transfer excited) state, *i.e.* {Q*, ArH} ↔ {Q$^{\bullet-}$, ArH$^{\bullet+}$}. Indeed, the largest value of K_{EC} in Chart 3 obtains for the **CX***/HMB pair with $\Delta G_{es} = 0$ to allow optimal mixing[45] of {**CX***, HMB} for which $E_T = 2.13$ eV[39] with the isoenergetic ion-pair state {**CX**$^{\bullet-}$, HMB$^{\bullet+}$} with an energy of $E°_{HMB} - E°_{CX} = 2.13$ eV.[46]

C. Formation Enthalpies of CT Complexes. The energetics for the formation of ground-state EDA complexes and excited-state encounter complexes of quinones and aromatic donors are evaluated by the enthalpy of formation ΔH_{EDA} and ΔH_{EC} from the temperature dependence of the formation constants K_{EDA} and K_{EC}, respectively. The value of ΔH_{EC} for the [**CX***, DUR] encounter complex in acetonitrile (as evaluated in this study) is comparable to that previously reported for the [**CA***, MES] exciplex in carbon tetrachloride.[19c] Furthermore, these enthalpies of formation fall in essentially the same energy range as those of the ground-state EDA complexes of the related fluoranil acceptor (see **FA** in Chart 4).[47] In all cases, complex formation is only slightly exothermic, and ΔH_{EC} and ΔH_{EDA} are comparable to formation enthalpies arising from mostly van der Waals forces.[48] This finding may seem somewhat anomalous if one considers the significantly different charge-transfer character of the (excited-state) encounter complex relative to the (ground-state) EDA complex as evaluated by the $(b/a)^2$ ratio for the degree of charge transfer in the Mulliken formulation (*vide supra*). For example, the latter can be evaluated directly from the enthalpy and charge-transfer data as $(b/a)^2 \simeq -\Delta H_{EDA}/h\nu_{CT}$ (evaluated in Chart 4 and Table 4);[49] and the "degree of

Chart 4. Formation Enthalpies of Charge-Transfer Complexes[19c,47]

Q/ArH	solvent	$\Delta H_{EC,EDA}$, kcal mol^{-1}
CX*/DUR	CH_3CN	−5.6
CA*/MES	CCl_4	−7.7
FA/MES	CCl_4	−3.0
FA/DUR	CCl_4	−3.9
FA/HMB	CCl_4	−5.4

(41) (a) The broad charge-transfer absorptions in the near IR are reminiscent of those found in other donor/acceptor pairs with an energy gap between the oxidation potential of the donor and the reduction potential of the acceptor close to zero.[41b] (b) Badger, B.; Brocklehurst, B. *Trans. Faraday Soc*. **1969**, *65*, 2576, 2582, 2588. For charge-resonance absorptions in mixed-valence metal complexes, see: Curtis, J. C.; Meyer, T. J. *Inorg. Chem*. **1982**, *21*, 1562. Curtis, J. C.; Meyer, T. J. *J. Am. Chem. Soc*. **1978**, *100*, 6284.

(42) The data in Table 2 are for the **CX**/HMB complex; the solvent polarity is the transition energy of solvatochromic absorption bands. See: (a) Dimroth, K.; Reichardt, C.; Siepmann, T.; Bohlmann, F. *Liebigs Ann. Chem*. **1963**, *661*, 1. (b) Reichardt, C. *Solvents and Solvent Effects in Organic Chemistry*; VCH: New York, 1988.

(43) Foster, R. *Organic Charge-Transfer Complexes*; Academic Press: New York, 1969; p 182.

(44) Formation constants obtained in dichloromethane. ΔG_{gs} represents the energy gap between the oxidation potential of the donor and the reduction potential of the acceptor, *i.e.* $\Delta G_{gs} = E°_{ox} - E°_{red}$. ΔG_{es} represents the energy gap between excited quinone (E_T) and the ion-pair state {A$^-$, D$^+$}, and is thus equivalent to the driving force (ΔG_{ET}) defined in eq 4. Thus, the excited and ground state are related by $\Delta G_{es} = \Delta G_{gs} - 2.13$ eV.

(45) See: Weller, A. in ref 7, p 23.

(46) The electrostatic work term is taken to be constant.

(47) Foster, R. *Organic Charge-Transfer Complexes*; Academic Press: New York, 1969; p 210.

(48) Ben-Naim, A. *J. Chem. Phys*. **1971**, *54*, 1387.

(49) (a) Ketelaar, J. A. A. *J. Phys. Radium* **1954**, *15*, 197. (b) Rabie, U. M.; Patel, B. P.; Crabtree R. H.; Mahmoud, M. R. *Inorg. Chem*. **1997**, *36*, 2236.

Chart 5

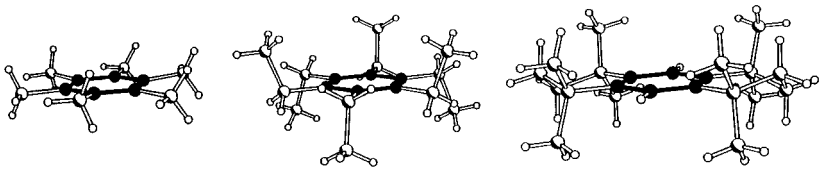

	HMB	HEB	OMA
Oxidation Potential (vs. SCE)	1.62 V	1.59 V	1.84 V
van der Waal Thickness (2r)	4.0 Å	6.4 Å	6.4 Å

charge transfer" is found to be 0.3 in the encounter complex, but only 0.05 in the EDA complex. Thus, the formation enthalpies are rather insensitive to the charge-transfer character of the excited encounter complex relative to the ground-state complex, especially at the limited levels of the degree of charge transfer shown by quinone/aromatic donor−acceptor pairs.

D. Steric Requirements for Complex Formation. The structural parallel between the EDA (ground-state) complex and the encounter (excited-state) complex is further underscored by the sharp differentiation of electron-rich aromatic donors of different steric sizes. For example, hexamethylbenzene readily forms the 1:1 EDA complex with chloranil in Table 4, in which the charge-transfer absorption derives from the $\pi-\pi$ interaction of the donor−acceptor pair at an intermolecular distance of $d = 3.5$ Å in structure **A**, established by X-ray crystallography.[50]

A.

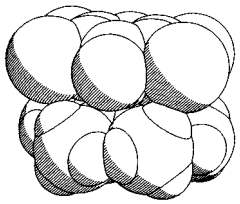

The inability of either hexaethylbenzene (HEB) or octamethyloctahydroanthracene (OMA) to show any signs of complex formation (despite oxidation potentials comparable to those of hexamethylbenzene or durene) can be ascribed to steric interference by the pendant methyl groups, as shown by comparison of the PLUTO structures in Chart 5, that discourage the close cofacial approach of the quinone acceptor to the benzenoid chromophore.[50]

The same steric discrimination is shown in the encounter (excited-state) complex. Thus, hexamethylbenzene forms the strongest encounter (excited-state) complexes, as judged by the intense near-IR bands (Figure 3) and by the large values of K_{EC} in all solvents (Table 2). By contrast, neither HEB nor OMA shows any indication of the encounter complex with either chloranil or dichloroxyloquinone, as deduced by the absence of near-IR absorption bands and by the remarkably linear k_{obs} *vs* [D] plots, even to high donor concentrations.[51] Finally, the larger formation constants in Table 2 indicate that the donor−acceptor pair moves closer together in the excited state (compared to $d = 3.5$ Å in the ground-state EDA complex) to form a rather tight complex with a strong overlap of the π-networks and enhanced degree of charge transfer, as evaluated by the $(b/a)^2$ values (*vide supra*).[52]

IV. Electron Transfer in the Direct Evolution of the Encounter Complex to Ion-Radical Pairs. The temporal evolution of the encounter complex (EC) by electron transfer directly to the ion-radical pair [$Q^{\bullet-}$, $ArH^{\bullet+}$] is established by the spectral changes in Figure 4. Thus, the first-order decays of the twin (near-IR and 500-nm) bands of [Q*, ArH] occur simultaneously with the first-order growth of the diagnostic 430-nm band of $Q^{\bullet-}$ in acetonitrile, *i.e.*[53]

$$[Q^*, ArH] \xrightarrow{k_{ET}} [Q^{\bullet-}, ArH^{\bullet+}] \qquad (6)$$

both within 10 ns, as described by the common values of the first-order rate constant k_{ET} in Table 2. However, the formation of the ion radicals as a contact ion pair could not be rigorously distinguished from a pair of solvated ion radicals, owing to their rapid dissociation, *i.e.*

$$\underset{\text{contact ion pair}}{[Q^{\bullet-}, ArH^{\bullet+}]} \xrightarrow[CH_3CN]{k_{diss}} \underset{\text{solvated ion radicals}}{Q^{\bullet-}, ArH^{\bullet+}} \qquad (7)$$

which is known to occur with first-order rate constants $k_{diss} > 10^9$ s^{-1} in polar solvents such as acetonitrile.[54] Although the spectral indistinguishability of contact and solvated ion-radical pairs[55] precludes the kinetic separation of k_{ET} and k_{diss}, we infer from the observed time scales that they arise from sequential (stepwise) and not simultaneous events, *i.e.* rate-limiting electron transfer followed by very fast ion separation.

In the less polar solvents (chloroform, dichloromethane, etc.), the first-order decay of the encounter complex takes up to 160 ns, as shown by the rate constants k_{ET} in the range of 10^7-10^8 s^{-1} in Table 2. The roughly 10-fold factor in rate difference

(50) (a) Harding, T. T.; Wallwork, S. C. *Acta Crystallogr*. **1955**, *8*, 787. (b) The optimum intermolecular distance in EDA complexes is the van der Waals separation of 3.5 Å.[38] Thus, the van der Waals radii of HEB and OMA of $r = 3.2$ Å exceed that for sufficient overlap of their π-chromophores with that of the quinone acceptors.

(51) For the effects of steric hindrance on exciplex formation, see: Jacques, P.; Allonas, X.; Suppan, P.; Von Raumer, M. *J. Photochem. Photobiol. A: Chemistry* **1996**, *101*, 183. See also: Zacchariasse, K. in ref 7, p 286.

(52) (a) Kim, E. K.; Kochi, J. K. *J. Am. Chem. Soc*. **1991**, *113*, 4962. (b) Friedrich, H. B.; Person, W. B. *J. Chem. Phys.* **1966**, *44*, 2161. (c) Kampar, V. E.; Valtere, S. P.; Neilands, O. Y. *Theor. Exp. Chem.* **1978**, *14*, 288.

(53) The stoichiometry of the electron-transfer reaction demands that $ArH^{\bullet+}$ is cogenerated with the quinone anion-radical $Q^{\bullet-}$. However, the absorption bands of $ArH^{\bullet+}$ are weak and, in most cases, obscured by the strong absorption of $Q^{\bullet-}$. See: refs 28 and 29.

(54) (a) Mattes, S. L.; Farid, S. *J. Am. Chem. Soc*. **1983**, *105*, 1396. (b) Knibbe, H.; Rehm, D.; Weller, A. *Ber. Bunsenger*. **1968**, *72*, 257. (c) Ojima, S.; Miyasaka, H.; Mataga, N. *J. Phys. Chem.* **1990**, *94*, 7534. (d) Hubig, S. M. *J. Phys. Chem*. **1992**, *96*, 2903.

(55) Arnold, B. R.; Atherton, S. J.; Farid, S.; Goodman, J. L.; Gould, I. R. *Photochem. Photobiol*. **1997**, *65*, 15. See also: Mataga *et al*. in ref 54c and Hubig in ref 54d.

Chart 6. Driving-Force Dependence of Electron Transfer[58]

Q/ArH	ΔG_{ET} (kcal mol^{-1})	k_{ET} (10^7 s^{-1})
CA/XYL	−2.1	8.0
CA/MES	−0.9	3.6
CX/HMB	0	11
CX/DUR	4.8	2.7

between acetonitrile and chloroform is consistent with the increased stabilization of ion radicals in the more polar medium. Even more striking is the spectral evolution of the encounter complex to yield the protonated quinone anion radical (Q-H$^{\bullet}$), as the electron-transfer product first observed in chloroform (see Figure 5). In such a medium of low polarity, we expect ion dissociation (k_{diss}) in eq 7 to be substantially slower than that in acetonitrile, which allows the fast proton transfer (k_H) within the ion-radical pair to compete effectively, *i.e.*[56]

$$\underset{\text{contact ion pair}}{[Q^{\bullet-}, ArH^{\bullet+}]} \xrightarrow[CHCl_3]{k_H} \underset{\text{radical pair}}{Q\text{-}H^{\bullet}, Ar^{\bullet}} \quad (8)$$

Such a stepwise process from the contact ion pair is confirmed by the pronounced salt effect induced by the added inert salt TBA^+ PF_6^- which effects ion-radical (pair) separation,[57] *i.e.*

$$[Q^{\bullet-}, ArH^{\bullet+}] + TBA^+ PF_6^- \rightleftarrows Q^{\bullet-}, TBA^+ + ArH^{\bullet+}, PF_6^- \quad (9)$$

The effectiveness of the ion-pair exchange in eq 9 is demonstrated by the spectral decay of the transient intermediate (in chloroform containing added salt) to afford the quinone anion radical ($\Phi_{Q^{\bullet-}} = 0.7$) and not Q-H$^{\bullet}$, as observed in the absence of salt (Figure 5). The exchange in eq 9 efficiently separates the ion radicals and thus effectively precludes the proton transfer within the contact ion pair according to eq 8. Importantly, the kinetics study in Figure 7 demonstrates that the salt effect is limited to the behavior of the *contact ion pair* following the rate-limiting electron transfer, since all the kinetic parameters associated with the encounter complex (k_2, K_{EC}, and k_{ET}) are singularly unaffected by the added salt in Table 2.

The electron-transfer rates within the encounter complex in eq 6 are experimentally represented by the value of k_{ET} in Chart 6 measured at different driving forces ΔG_{ET}, as defined in eq 4.[58] Although we note a slight increase in k_{ET} with increasing exergonicity of the electron transfer from the aromatic donor to Q*, the magnitude of the trend is clearly insufficient to quantitate. Indeed, such a mild ΔG_{ET} dependence is typically observed for back-electron-transfer rates upon the photoexcitation of charge-transfer complexes.[8,59,60]

Time-resolved spectroscopy thus demonstrates that the encounter complex (EC) plays a pivotal role in effecting the electron transfer from aromatic donors to Q*, i.e.

$$Q^* + ArH \overset{K_{EC}}{\rightleftharpoons} [Q^*, ArH] \xrightarrow{k_{ET}} [Q^{\bullet-}, ArH^{\bullet+}] \quad (10)$$

The direct intervention of the encounter complex in the electron transfer from aromatic donors (ArH) to quinones (Q*) according to eq 10 is based on three independent lines of experimental evidence involving (a) the spectroscopic observation of distinctive far red-shifted bands in the near-IR region in Figures 2 and 3, (b) the curved k_{obs} vs [D] plots in Figure 6, and (c) the lack of temperature dependence of the electron-transfer rate constants of k_2 in Table 3.[61]

V. Mechanistic Significance of the Encounter Complex to Bimolecular Electron Transfers. The use of quinone as the acceptor to examine the dynamics of electron transfer is a particularly felicitous choice since the preassociation is spectrally observable both in its excited state Q* (by the near-IR bands in Figures 2 and 3) and in its ground state Q (by the visible spectrum in Figure 8). Indeed, the parallel pathways for electron transfer to Q* and to Q from the graded series of aromatic donors (D) can be directly compared by emphasizing the overall thermodynamic relationships among the various species, as diagrammatically presented in Scheme 1. [Note that the relative energy levels are somewhat arbitrary, and the spin multiplicities are not included.]

Scheme 1

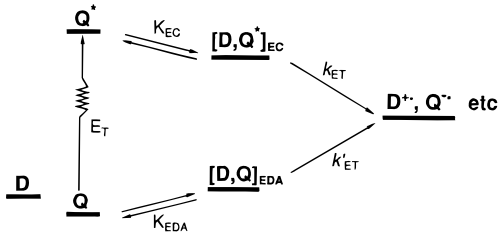

The electron-transfer mechanism as depicted in the lower (ground-state) manifold in Scheme 1 proceeds via the preequilibrium formation of the electron donor−acceptor complex $[D,Q]_{EDA}$ which has been elaborated in earlier reports.[62] In this study, laser photoactivation spontaneously generates Q*, which resides at an energy level of $E_T = 50$ kcal mol^{-1} above that of Q, and this necessitates the use of fast (time-resolved) spectroscopy to directly measure its fast temporal evolution via the encounter complex $[D,Q^*]_{EC}$, as presented in the upper (excited-state) manifold in Scheme 1. Otherwise, Q and Q* follow the same overall electron-transfer (kinetics) behavior; and the basic difference is in the *energetics*—the encounter complex lying at substantially higher energy levels than the EDA complex. As a result, the driving force for electron transfer from $[D,Q^*]_{EC}$ is highly exergonic under conditions in which that from $[D,Q]_{EDA}$ is endergonic.

The encounter complex and the EDA complex both represent the preorganization of the reactants prior to electron transfer,[63] as underscored by the intimate cofacial juxtaposition of the donor and acceptor for optimal overlap of their π-orbitals, as seen in the side and top perspectives A_S and A_T below.[50]
In such complexes, the electronic coupling of the donor/acceptor moieties is given roughly by the degree of charge-transfer $(b/a)^2$, which reflects the contribution from the ionic or $[D^{\bullet+}, Q^{\bullet-}]$ form.[37] Thus, the reasonable values of $(b/a)^2 \simeq 0.3$ in $[D,Q^*]_{EC}$

(56) Fast proton transfer from polymethylbenzene cation−radicals is known to occur with rate constants of about 10^8 s^{-1}. See: (a) Masnovi, J. M.; Sankararaman, S.; Kochi, J. K. *J. Am. Chem. Soc.* **1989**, *111*, 2263. (b) Schlesener, C. J.; Amatore, C.; Kochi, J. K. *J. Am. Chem. Soc.***1984**, *106*, 7472. (c) See also: Jones *et al*. in ref. 18.

(57) Yabe, T.; Kochi, J. K. *J. Am. Chem. Soc.* **1992**, *114*, 4491. See also: Bockman, T. M.; Kochi, J. K. in ref 17c.

(58) In the gas phase, the driving force to move an electron from the HOMO of the donor to the LUMO of the acceptor is equal to the difference of the ionization potential and the electron affinity of the donor and the acceptor, respectively. In solution, solvation terms and coulombic work terms must also be considered.[22,23]

(59) Asahi, T.; Ohkohchi, M.; Mataga, N. *J. Phys. Chem.* **1993**, *97*, 13132.

(60) Hubig, S. M.; Bockman, T. M.; Kochi, J. K. *J. Am. Chem. Soc.* **1996**, *118*, 3842.

(61) For the mechanistic deductions of this unusual temperature effect, see: Baggott in ref 13c.

(62) (a) For a review, see: Kochi, J. K. *Acta Chem. Scand.* **1990**, *44*, 409. (b) We take the electronic coupling of the donor and acceptor in the encounter complex to be symptomatic of an inner-sphere complex, since such an interaction is minimal in an outer-sphere complex.[3] The characteristics of inner-sphere *vs* outer-sphere behavior in bimolecular electron-transfer reactions will be discussed in a subsequent paper.[35]

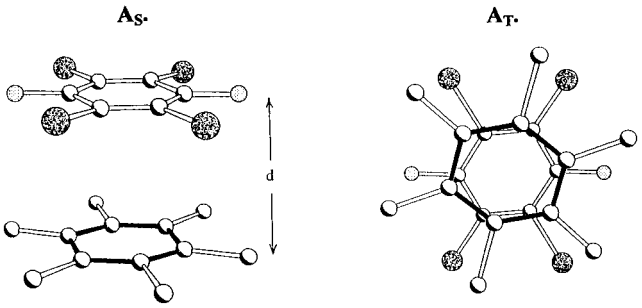

point to an encounter complex that is already predisposed significantly toward electron transfer.[63b] As such, the charge-transfer character of the encounter complex provides the rationale for its intermediacy in electron transfer,[62b] especially since the prior association step occurs at a diffusion-controlled rate.

Summary and Conclusions

Time-resolved (ps → μs) spectroscopy reveals three distinct and sequential events (together with the attendant intermediates) in the bimolecular electron transfer from aromatic donors (D) to photoactivated quinones (Q*). Initially, the redox-active acceptor Q* is formed within the 25-ps laser pulse with unit quantum yield. Subsequently, on the early nanosecond time scale, the diffusion-controlled association of Q* with the aromatic donors leads to the encounter complex $[D,Q^*]_{EC}$. Finally, on the ns/μs time scale, the internal electron transfer (k_{ET}) within the encounter complex results in the formation of the ion-radical pair $[D^{\bullet+}, Q^{\bullet-}]$ with unit efficiency in acetonitrile. Thus, the encounter complex and the ion-radical pair are neither the same nor alternative (solvent-dependent) intermediates in bimolecular electron transfer; but their formation and decay can be individually monitored on distinct time scales in polar solvents. Moreover, the observation of ion radicals ($Q^{\bullet-}$) even in solvents of low polarity (upon the addition of salt) confirms the generality of this sequence of ET intermediates—independent of the polarity of the reaction medium.

The encounter complex is characterized by strong charge-transfer interactions between the donor/acceptor moieties that are revealed spectroscopically by broad absorptions in the near-IR region and thermodynamically by large formation constants K_{EC} as compared to those of (ground-state) EDA complexes. Apart from differences in energy content, however, photoactivated encounter complexes and EDA complexes exhibit quite similar structural and charge-transfer properties, and they play analogous roles as preassociation intermediates in photoactivated and ground-state electron-transfer processes, respectively, as pictorially depicted in Scheme 1. Both complexes thus represent experimentally observable examples of precursor complexes of the type theoretically postulated for bimolecular (adiabatic) electron transfer.[2,3]

Experimental Section

Materials. Hexaethylbenzene (Acros), hexamethylbenzene, and durene (Aldrich) were recrystallized from ethanol and heptane. Mesitylene (Aldrich) and *p*-xylene (Aldrich) were purified by fractional distillation. Tetrachloro-*p*-benzoquinone (chloranil, Aldrich) was sublimed *in vacuo* and recrystallized from benzene.

Synthesis of 2,5-Dichloro-3,6-dimethyl-1,4-benzoquinone (CX). Chlorination of 2,5-dimethyl-1,4-dimethoxybenzene[64] with sulfuryl chloride in the presence of a catalytic amount of iodine in dichloromethane afforded 2,5-dichloro-3,6-dimethylhydroquinone dimethyl ether quantitatively, which was readily oxidized to the corresponding quinone with excess nitric acid (63%) in an excellent yield of 88%. Mp 55 °C; ^{1}H NMR δ 2.24 (s, 6H); ^{13}C NMR ($CDCl_3$) 14.45, 140.95, 142.16, 177.45. GC-MS *m/z* 205 (M^+), calcd for $C_8H_6O_2Cl_2$. Anal. Calcd for $C_8H_6O_2Cl_2$: C, 46.85; H, 2.95; Cl, 34.58. Found: C, 46.67; H, 2.90; Cl, 34.43. Dichloromethane, acetonitrile, chloroform, and carbon tetrachloride were purified according to standard procedures.[65]

Instrumentation. The UV−vis absorption spectra were recorded on a Hewlett-Packard 8453 diode-array spectrometer. For the nanosecond-laser experiments, the third-harmonic (355 nm) output of a Q-switched Nd:YAG laser (10-ns fwhm, 22 mJ)[66] was used to generate the triplet quinones. The picosecond time-resolved pump-probe experiments were carried out with the third-harmonic (355 nm) output of a mode-locked Nd:YAG laser (25 ps fwhm, 10 mJ).[66] The one-electron oxidation potentials of the arene donor were determined by cyclic voltammetry with use of a BAS 100A electrochemical analyzer. All potentials in Chart 1 were measured in dichloromethane containing 10% trifluoroacetic acid and 0.1 M tetra-*n*-butylammonium hexafluorophosphate.[22] The standard calomel electrode was used as reference.

Determination of the Formation Constants of the EDA Complexes. A 0.001 M solution of quinone was placed in a 1-cm quartz cuvette equipped with a side arm and a Schlenk adapter under an argon atmosphere. Known amounts of arene donor were added in small increments, and the growth of the charge-transfer absorption band was monitored at several wavelengths. The absorbance data were then evaluated with the aid of the Benesi−Hildebrand correlation,[36] *i.e.* $[Q]/A_{CT} = \epsilon_{CT}^{-1} + (K_{EDA}\epsilon_{CT}[D])^{-1}$, where [Q] was the quinone concentration, A_{CT} was the charge-transfer absorbance (monitored at a wavelength (λ_{CT}) within the CT absorption band), ϵ_{CT} was the extinction coefficient of the EDA complex at the monitoring wavelength λ_{CT}, K_{EDA} was the formation constant of the EDA complex, and [D] was the donor concentration. Thus, the linear plot of $[Q]/A_{CT}$ *versus* the reciprocal donor concentration exhibited a slope of $(K_{EDA}\epsilon_{CT})^{-1}$ and an intercept of ϵ_{CT}^{-1} from which the values of K_{EDA} and $K_{EDA}\epsilon_{CT}$ in Table 4 were extracted with correlation coefficients $R > 0.999$. Each Benesi−Hildebrand experiment was carried out twice to ensure reproducibility within the least-squares error bars.

Determination of the Maximum Extinction Coefficient and the Quantum Yield of Triplet 2,5-Dichloroxyloquinone. The absorption spectrum of the triplet state of 2,5-dichloroxyloquinone (**CX**) exhibits a maximum at 500 nm (see Figure 1B). To determine the maximum triplet extinction coefficient ($\epsilon_{T,\,500}$), we carried out an energy-transfer experiment to generate triplet **CX** from triplet benzophenone[67] as follows: Benzophenone (13.8 mg, 0.015 M) and **CX** (1.1 mg, 0.001 M) were dissolved together in acetonitrile (5 mL) under an argon atmosphere. Upon laser excitation (Nd:YAG, 10 ns, 355 nm), the transient absorption spectra recorded between 0 and 400 ns showed the decay of triplet benzophenone in the wavelength region between 500 and 600 nm and the growth of triplet **CX** in the region between 400 and 500 nm. The transient absorbance monitored at 500 nm did not change over the same time period. This isosbestic point at 500 nm indicated that triplet benzophenone and triplet **CX** exhibit the same extinction coefficient at this wavelength ($\epsilon_{T,\,500}$). We determined the extinction coefficient of triplet benzophenone in acetonitrile at 500 nm to be 5300 M^{-1} cm^{-1} by quantitative comparison of triplet benzophenone spectra in acetonitrile and benzene.[25] On the basis of the isosbestic point at 500 nm in the benzophenone/**CX** transient spectra, we conclude that the maximum extinction coefficient of 2,5-dichloroxyloquinone in acetonitrile at 500 nm amounts to $\epsilon_{T,\,500} = 5300$ M^{-1} cm^{-1}. The

(63) (a) It has been long recognized in enzymology that an analogous preorganization in the form of reversible (enzyme/substrate) complexation greatly facilitates processes that are otherwise unfavorable (and slow), and it is thus not unexpected that eq 2 has essentially the same form as the Michaelis−Menten equation (see: Stryer, L. *Biochemistry*, Freeman: San Francisco, 1985; pp 103−185). (b) The enhanced degree of charge transfer in $[D,Q^*]_{EC}$ in lowering the energy of the transition state for the exergonic electron transfer in the excited-state manifold (relative to that in $[D,Q]_{EDA}$ for the ground-state manifold compared in Scheme 1) accords with the Hammond postulate [Hammond, G. S. *J. Am. Chem. Soc.* **1995**, *77*, 334].

(64) Rathore, R.; Bosch, E.; Kochi, J. K. *Tetrahedron* **1994**, *50*, 6727.

(65) Perrin, D. D.; Armarego, W. L. F. *Purification of Laboratory Chemicals*, 3rd ed.; Pergamon: Oxford, 1988.

(66) Bockman, T. M.; Karpinski, Z. J.; Sankararaman, S.; Kochi, J. K. *J. Am. Chem. Soc.* **1992**, *114*, 1970.

(67) Bensasson, R.; Land, E. J. *Trans. Faraday Soc.* **1971**, *67*, 1904.

triplet quantum yield of 2,5-dichloroxyloquinone was determined by transient actinometry.[25] Thus, a solution of benzophenone in benzene and a solution of dichloroxyloquinone in acetonitrile, both with matched absorbance at 355 nm, were excited with the Q-switched Nd:YAG laser (10 ns, 355 nm), and the transient absorbances extrapolated to time $t = 0$ were measured at 525 and 500 nm, respectively. The triplet quantum yield of dichloroxyloquinone $\Phi_{T,CX}$ was then determined according to the following: $\Phi_{T,CX} = (A_{500,CX}/A_{525,BP})(\epsilon_{525,BP}/\epsilon_{500,CX})\Phi_{T,BP}$, where $A_{500,CX}$ and $A_{525,BP}$ were the transient absorbances of **CX** and benzophenone at 500 and 525 nm, respectively, $\epsilon_{525,BP}$ and $\epsilon_{500,CX}$ were the triplet extinction coefficients of benzophenone in benzene and **CX** in acetonitrile at 525 and 500 nm, respectively, and $\Phi_{T,BP}$ was the triplet quantum yield of benzophenone in benzene. Taking $\epsilon_{525,BP} = 7220$ M^{-1} cm^{-1},[25] $\epsilon_{500,CX} = 5300$ M^{-1} cm^{-1}, and $\Phi_{T,BP} = 1.0$,[68] we obtained a triplet quantum yield of $\Phi_{T,CX} = 1.0 \pm 0.05$.

(68) Moore, W. M.; Hammond, G. S.; Foss, R. P. *J. Am. Chem. Soc.* **1961**, *83*, 2789.

Determination of Free-Ion Yields. The free-ion yields in acetonitrile and chloroform (with added salt) were determined by the same method as described above in detail for the determination of the triplet quantum yield. Thus, benzophenone in benzene was used as the transient actinometer[25] and samples of the quinone/donor combinations and of benzophenone with matching absorbances at 355 nm were photoexcited with the 10-ns Nd:YAG laser. The free-ion yields were then determined by quantitative comparison of the maximum absorbance of triplet benzophenone at 525 nm ($\epsilon = 7220$ M^{-1} cm^{-1})[25] and the maximum absorbance of chloranil anion radical at 450 nm ($\epsilon = 9700$ M^{-1} cm^{-1})[30] or **CX** anion radical at 430 nm ($\epsilon = 6800$ M^{-1} cm^{-1}).[28]

Acknowledgment. We thank T. M. Bockman for many helpful discussions and the National Science Foundation and the R. A. Welch Foundation for financial support.

JA971188Y